Impedance Matching and Power Division using Impedance Inverter for Wireless Power Transfer via Magnetic Resonant Coupling

Koh Kim Ean
Student Member, IEEE
The University of Tokyo
5-1-5 Kashiwanoha
Kashiwa, Chiba
277-8561, Japan
koh@hori.k.u-tokyo.ac.jp

Beh Teck Chuan
Engineer
GE Healthcare
4-7-127 Asahigaoka
Hino, Tokyo
191-8503, Japan
teckchuan.beh@ge.com

Takehiro Imura
Member, IEEE
The University of Tokyo
5-1-5 Kashiwanoha
Kashiwa, Chiba
277-8561, Japan
imura@hori.k.u-tokyo.ac.jp

Yoichi Hori
Fellow, IEEE
The University of Tokyo
5-1-5 Kashiwanoha
Kashiwa, Chiba
277-8561, Japan
hori@k.u-tokyo.ac.jp

***Abstract*—Future applications of wireless power transfer will include powering various devices in a room, charging electric vehicles in a parking area, charging moving robots and so on. Therefore practical wireless power transfer must be able to support complicated configurations for example combination of multi-receiver and repeaters. Many past works have discussed on methods for improving efficiency and more recently extended the methods to multi-receiver system. However controllable power division among receivers is also an important feature as receivers nearer to the transmitter tend to absorb more power compared to further ones. In this paper, a new impedance matching and power division method utilizing impedance inverters only at receiver sides is proposed. The mathematical equations in the proposed method are then generalized for arbitrary number of receivers and arbitrary number of repeaters.**

***Index Terms*—Circuit analysis, Inverters, Impedance, Impedance Matching, Magnetic circuits, Resonance, RLC circuits.**

NOMENCLATURE

ω_0	Resonant angular frequency.
C_0	Capacitance of transmitter.
L_0	Inductance of transmitter.
R_0	Power supply termination resistance.
$k_{\mathrm{e}0}$	External coupling coefficient of transmitter.
C_{ij}	Capacitance of ith coil in jth transmission path.
L_{ij}	Inductance of ith coil in jth transmission path.
k_{ij}	Coupling coefficient of ith coil with $(i-1)$th coil in jth transmission path.
$L_{\mathrm{m}ij}$	Mutual Inductance of ith coil with $(i-1)$th coil in jth transmission path.
K_{ij}	Coupling of ith coil with $(i-1)$th coil in jth transmission path represented with characteristic impedance.
$R_{\mathrm{L}j}$	Load resistance of jth receiver.
$k_{\mathrm{e}j}$	External coupling coefficient of jth receiver.
$K_{\mathrm{e}j}$	Inverter's characteristic impedance in jth receiver.
$C_{\mathrm{e}j}$	Capacitance in jth receiver's inverter circuit.
L_{ej}	Inductance jth receiver's inverter circuit.
η_0	Loss in ith transmitter coil.
η_{ij}	Loss in ith coil in jth transmission path.
η_{ej}	Loss in inductor of jth receiver's inverter circuit.

I. INTRODUCTION

An ideal wireless power transfer must be able to transfer power efficiently regardless of the receiving end in the effective region. However magnetic resonant coupling method is efficient only in a fixed distance and orientation. When the receiver is moved away from its optimal operating point, the efficiency falls off rapidly [1]. Furthermore, in a wireless power transfer consist of multiple receivers, receivers nearer to the transmitter tend to absorb more power [2]. Many past papers have proposed different ways to resolve the efficiency issue but not on power distribution.

Paper [3]-[5] explore the possibilities of multi-receiver system using either equivalent circuit or coupled mode theory. Efficiency analysis for different conditions is provided but methods for improving efficiency and power distribution are not proposed. Often wireless power transfer is analyzed using equivalent circuit [3], [6]-[11], however the equations for system with more coils quickly becomes complex or rigorous to be analyzed [3], [9]. Therefore, band-pass filter representation is proposed by [12], [13]. The design equations are very simple even with many repeaters added in the power transfer system. However the method is impractical due to inapplicable to multi-receiver and all the coils' positions need to be controllable.

Other attempts include adding and adjusting a medium coil to improve the transfer efficiency [14], [15]. The method however is limited to specific case. Frequency tracking method where the frequency of the source is varied for different conditions has also been proposed [1], [16], [17]. In practical applications, the wireless power transfer should stay inside an allowable industrial, scientific and medical band which is narrow. Therefore, tuning frequency is not a feasible method for wireless power transfer. In [7], [18], impedance matching circuit is inserted in the transmitter side based on equivalent circuit model. Transfer efficiency is optimized regardless of the receiving end. However controllable power distribution is not possible using this method.

In a multi-receiver system, not only the transfer effi-

ciency is important but also the power distribution among the receivers. Power distribution depends on both the load impedances and the relative positions of the receivers to the transmitter. Assuming identical load connected to each receiver, the receiver nearer to the transmitter tends to absorb most of the power while the further receiver may not obtain enough to function properly. In this paper, method for impedance matching and controllable power division for a 13.56 MHz system [19], [20] is proposed. The design equations are derived and then generalized for arbitrary number of receivers and arbitrary number of repeaters. Simulations using LTspice and experiments are performed to validate the new method.

II. Multi-receiver and Repeater Wireless Power Transfer

A. Impedance Inverter

Impedance inverter is a circuit which has input impedance inversely proportional to the impedance connected at the other end. There are many applications and many types of impedance inverter [21]. In this paper, impedance inverter is used to represent the couplings between coils and impedance matching.

Consider the equivalent circuit of one-transmitter and one-receiver wireless power transfer shown in Fig. 1. When coupling strength, k_{11} is expressed in mutual inductance terms [22], the equivalent circuit can be redrawn into Fig. 2 where:

$$k_{11} = \frac{L_{\mathrm{m11}}}{\sqrt{L_0 L_{11}}} \tag{1}$$

The components in the dashed rectangular formed an impedance inverter circuit and impedance Z_1, viewed from the transmitter towards the load is:

$$\begin{aligned} Z_1 &= -j\omega_0 L_{\mathrm{m11}} + [j\omega_0 L_{\mathrm{m11}} // (-j\omega_0 L_{\mathrm{m11}} + R_{\mathrm{L1}})] \\ &= \frac{(\omega_0 L_{\mathrm{m11}})^2}{R_{\mathrm{L1}}} \\ &= \frac{{K_{11}}^2}{R_{\mathrm{L1}}} \end{aligned} \tag{2}$$

Provided that the internal resistance of coils are small enough and can be ignored, and the system is in resonance. Therefore:

$$\begin{aligned} j\omega_0 L_0 + \frac{1}{j\omega_0 C_0} &\approx 0 \\ j\omega_0 L_{11} + \frac{1}{j\omega_{11} C_{11}} &\approx 0 \end{aligned} \tag{3}$$

Magnetic resonant coupling coils have low internal resistance [23]. For simplicity, small impedance of the resonators is omitted in the design equations and dissipation loss calculation is performed afterwards.

Term K_{11} is the characteristic impedance of inverter [24] in Fig. 2. Relating coupling coefficient, k_{11} in (1) and K_{11} in (2), inverter's characteristic impedance can be used

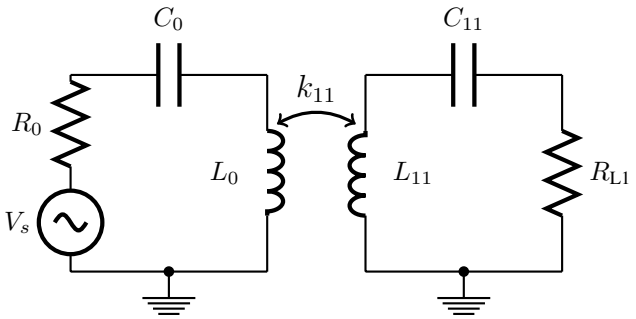

Fig. 1. One-transmitter and one-receiver wireless power transfer

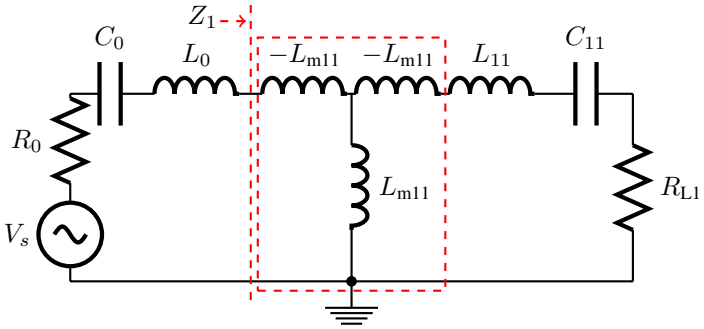

Fig. 2. Impedance inverter as coupling strength representation

to represent the coupling strength in between two coils.

$$\begin{aligned} K_{11} &= \omega_0 L_{\mathrm{m11}} \\ &= \omega_0 k_{11} \sqrt{L_0 L_{11}} \end{aligned} \tag{4}$$

The advantage of using inverter's characteristic impedance representation is equation of form (2) can be used to simplify impedance calculation in magnetic resonant circuit.

Besides coupling representation, inverter circuit is also used for impedance transformation. Fig. 3 is the same one-transmitter and one-receiver system in Fig. 1 except that an inverter circuit is implemented in between the receiver and load.

External coupling coefficient is defined as the ratio of the resonators' termination resistance to the resonators' "reactance slope parameter" [12][24]. External coupling coefficients of transmitter, k_{e0}, and the receiver, k_{e1} for the one-transmitter and one-receiver system before implementing load impedance transformation are:

$$k_{\mathrm{e0}} = \frac{R_0}{\omega_0 L_0} \qquad k_{\mathrm{e1}} = \frac{R_{\mathrm{L1}}}{\omega_0 L_{11}} \tag{5}$$

After impedance transformation using the inverter circuit in dashed rectangular of Fig. 3, the new k_{e1} is:

$$\begin{aligned} k_{\mathrm{e1}} &= \frac{{R_{\mathrm{L1}}}'}{\omega_0 L_{11}} \\ &= \frac{\left({K_{\mathrm{e1}}}^2 / R_{\mathrm{L1}}\right)}{\omega_0 L_{11}} \end{aligned} \tag{6}$$

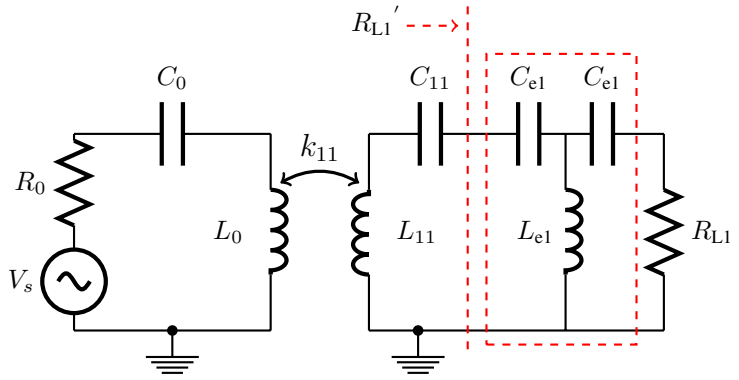

Fig. 3. Impedance inverter for impedance transformation

The derivation and calculation of required receiver's external coupling coefficients are given in subsequent sections.

The resonant coils used in magnetic resonant coupling are considered as lumped elements due to the diameter are smaller than one-tenth of a wavelength [25]. Therefore lumped inductors and capacitors are used in the impedance inverter circuit shown in the dashed rectangular in Fig. 3. The configuration is chosen so that the number of inductors can be minimized and the inverter circuit will be smaller. From (6), the required characteristic impedance of the inverter, K_{e1} is determined and is realised using inductor and capacitors with values [24]:

$$K_{e1} = \omega_0 L_{e1} = \frac{1}{\omega_0 C_{e1}} \tag{7}$$

B. System with Multi-receiver

Fig. 4 shows an equivalent circuit of a two-receiver wireless power transfer. Both receivers are coupled to the transmitter but cross coupling is not considered in this method. In actual applications, receivers are integrated into electric vehicles or other devices. The receivers therefore will not be overlapping and will be separated at least 10% of the largest dimension. In this case, cross coupling will be significantly weaker compared to the coupling with transmitter [26].

The external coupling coefficients of this two-receiver system before impedance transformation are:

$$k_{e0} = \frac{R_0}{\omega_0 L_0} \qquad k_{e1} = \frac{R_{L1}}{\omega_0 L_{11}} \qquad k_{e2} = \frac{R_{L2}}{\omega_0 L_{12}} \tag{8}$$

Assuming all the coils are similar and the power source is operating at their resonant frequency, the impedance of coils is therefore ignored in the design equations for simplification. Deducing from (2), (4):

$$\begin{aligned} Z_1 &= \frac{{K_{11}}^2}{R_{L1}} \\ Z_2 &= \frac{{K_{12}}^2}{R_{L2}} \\ K_{11} &= \omega_0 k_{11}\sqrt{L_0 L_{11}} \\ K_{12} &= \omega_0 k_{12}\sqrt{L_0 L_{12}} \end{aligned} \tag{9}$$

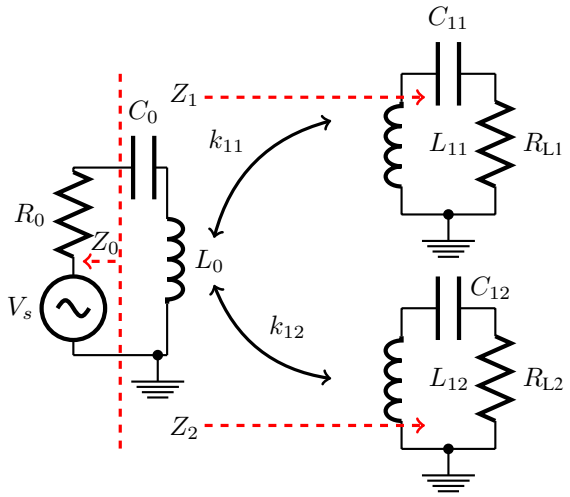

Fig. 4. Equivalent circuit of a two-receiver system

Where Z_1 is the impedance looking from transmitter to the first receiver in Fig. 4 and Z_2 is the impedance looking from transmitter to the second receiver. Substituting (8) into (9), the power supply's output impedance, Z_0, Z_1 and Z_2 in terms of coupling coefficients and external coupling coefficients are:

$$\begin{aligned} Z_0 &= R_0 = k_{e0}\omega_0 L_0 \\ Z_1 &= \frac{{k_{11}}^2}{k_{e1}}\omega_0 L_0 \\ Z_2 &= \frac{{k_{12}}^2}{k_{e2}}\omega_0 L_0 \end{aligned} \tag{10}$$

Circuit in Fig. 4 is redrawn into Fig. 5 with mutual inductance terms to derive impedance matching and power division equations. Deducing from (1):

$$k_{11} = \frac{L_{m11}}{\sqrt{L_0 L_{11}}} \qquad k_{12} = \frac{L_{m12}}{\sqrt{L_0 L_{12}}} \tag{11}$$

The current loop equations for Fig. 5 are given as:

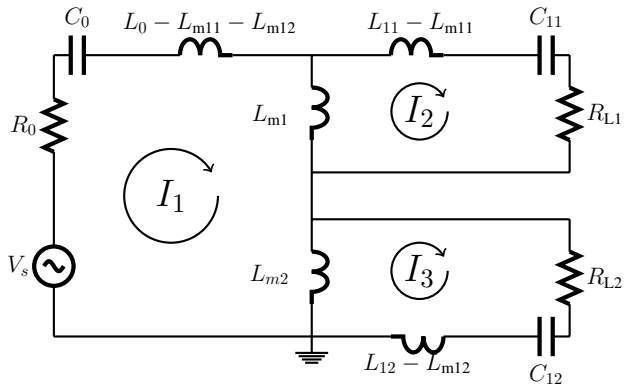

Fig. 5. Circuit of two-receiver wireless power transfer in terms of mutual inductance

$$\begin{aligned} V_s =& I_1 R_0 - I_2 j\omega_0 L_{m11} - I_3 j\omega_0 L_{m12} \\ 0 =& I_2 R_{L1} - I_1 j\omega_0 L_{m11} \\ 0 =& I_3 R_{L2} - I_1 j\omega_0 L_{m12} \end{aligned} \tag{12}$$

Solving current I_2 and I_3 in terms of I_1:

$$\begin{aligned} I_2 &= \frac{j\omega_0 L_{m11}}{R_{L1}} \times I_1 \\ I_3 &= \frac{j\omega_0 L_{m12}}{R_{L2}} \times I_1 \end{aligned} \tag{13}$$

Substituting (13) in the transmitter loop equation of (12), replacing load impedance with external coupling coefficient from (8) and mutual inductance with coupling coefficient from (11) :

$$\begin{aligned} \frac{V_s}{I_1} &= k_{e0}\omega_0 L_0 + \frac{{k_{11}}^2}{k_{e1}}\omega_0 L_0 + \frac{{k_{12}}^2}{k_{e2}}\omega_0 L_0 \\ &= Z_0 + Z_1 + Z_2 \end{aligned} \tag{14}$$

Equation (14) implies that circuit in Fig. 4 and Fig. 5 can be simplified into circuit shown in Fig. 6. The first term in (14) is the power supply's output impedance, the second term is impedance Z_1 and the third term is impedance Z_2 in Fig. 4. Using maximum power transfer theorem [22], impedance matching is achieved when:

$$\begin{aligned} Z_0 &= Z_1 + Z_2 \\ k_{e0} &= \frac{{k_{11}}^2}{k_{e1}} + \frac{{k_{12}}^2}{k_{e2}} \end{aligned} \tag{15}$$

Same current I_1 is flowing through impedance Z_1 and impedance Z_2 and both receivers are not coupled, therefore the power division ratio is:

$$\begin{aligned} P_1 &: P_2 \\ Z_1 &: Z_2 \\ \frac{{k_{11}}^2}{k_{e1}} &: \frac{{k_{12}}^2}{k_{e2}} \end{aligned} \tag{16}$$

where P_1 and P_2 are power across R_{L1} and power across R_{L2} respectively.

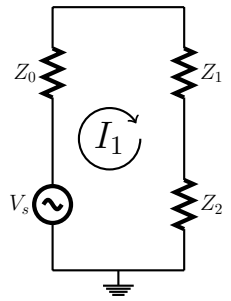

Fig. 6. Simplified two-receiver circuit

Power division ratio can also be derived using current flowing through each load. For system in Fig. 4 or Fig. 5, P_1 and P_2 are respectively:

$$\begin{aligned} P_1 &= |I_2|^2 R_{L1} \\ P_2 &= |I_3|^2 R_{L2} \end{aligned} \tag{17}$$

Again using (8), (11) and (13):

$$\begin{aligned} P_1 &= \frac{{k_{11}}^2}{k_{e1}} \times \omega_0 L_0 \times |I_1|^2 \\ P_2 &= \frac{{k_{12}}^2}{k_{e2}} \times \omega_0 L_0 \times |I_1|^2 \end{aligned} \tag{18}$$

The power division ratio, $P_1 : P_2$ is therefore once again agreeing with (16).

For controllable power division and impedance matching without having to change the coils' positions, impedance inverter circuit as shown in Fig. 3 is used for impedance transformation. The new external coupling coefficients of receivers after impedance transformation are:

$$\begin{aligned} k_{e1} &= \frac{{R_{L1}}'}{\omega_0 L_{11}} \\ &= \frac{({K_{e1}}^2/R_{L1})}{\omega_0 L_{11}} \end{aligned} \tag{19}$$

$$k_{e2} = \frac{{R_{L2}}'}{\omega_0 L_{12}} \tag{20}$$

$$= \frac{({K_{e2}}^2/R_{L2})}{\omega_0 L_{12}} \tag{21}$$

External coupling coefficient of transmitter, k_{e0} is fixed since impedance transformation is not implemented in the transmitter. For given coils' positions, the required external coupling coefficient of every receiver is calculated by solving (15) and (16) where $P_1 : P_2$ is the desired power division ratio.

C. System with Repeaters

Although wireless power transfer via magnetic resonant coupling is able to transmit power more efficiently compared to induction method, the transmittable distance is still limited to a few meters. This range is extendable using repeater coils. However as more coils are added into the system, existing equivalent circuit equations become complicated. Paper [7] resorts to search algorithms and

[9] uses computer aided design (CAD). Band-pass filter design method [12], [13] is simple but is impractical due to stringent conditions exerted by band-pass filter equations. In this paper, not only power division methods, but also new impedance matching method for wireless power transfer with repeaters is proposed. The new method combines the advantages of both existing equivalent circuit and band-pass filter method.

Consider the equivalent circuit of a wireless power transfer with a repeater coil in between transmitter and receiver shown in Fig. 7. Assuming impedance matching is to be carried out by transforming impedance Z_4.

$$Z_4 = Z_3 \tag{22}$$

The external couplings of this system before impedance transformation are:

$$\begin{aligned} k_{\mathrm{e}0} &= \frac{R_0}{\omega_0 L_0} \\ k_{\mathrm{e}1} &= \frac{R_{\mathrm{L}1}}{\omega_0 L_{21}} \end{aligned} \tag{23}$$

In order to satisfy (22), the required new $k_{\mathrm{e}1}$ is calculated. Assuming the system is in resonance and the impedance of all the coils is ignored. Using equation of form (2) to calculate impedance in Fig. (7):

$$\begin{aligned} Z_1 &= R_0 \\ Z_2 &= \frac{{K_{11}}^2}{Z_1} \\ Z_3 &= \frac{{K_{21}}^2}{Z_2} \end{aligned} \tag{24}$$

Deducing from (4):

$$\begin{aligned} K_{11} &= \omega_0 k_{11} \sqrt{L_0 L_{11}} \\ K_{21} &= \omega_0 k_{21} \sqrt{L_{11} L_{21}} \end{aligned} \tag{25}$$

Substituting (22), (23) and (25) into (24), the required external coupling of the receiver is:

$$k_{\mathrm{e}1} = k_{\mathrm{e}0} \times \frac{{k_{21}}^2}{{k_{11}}^2} \tag{26}$$

An inverter circuit can then be inserted into the receiver side, similarly to Fig. 3 to realise the required external coupling coefficients.

D. Generalized Equations for System with Both Multi-receiver and Repeaters

The equations derived in previous subsections are generalized for wireless power transfer with arbitrary number of repeaters and arbitrary number of receivers. Consider a wireless power transfer with m number of receivers and $n(j)-1$ number of repeaters in between jth receiver and transmitter in Fig. 8.

Firstly, external coupling coefficient of the transmitter, $k_{\mathrm{e}0}$ is broken down into m-number of parts:

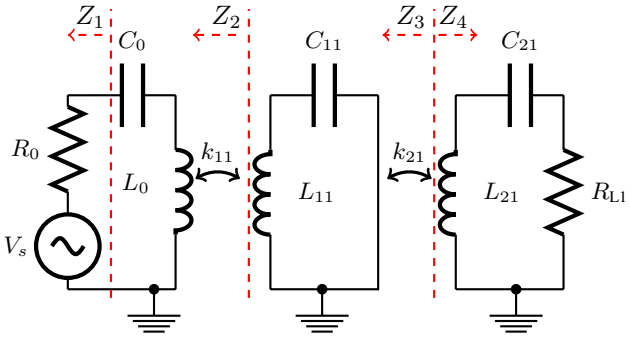

Fig. 7. Equivalent circuit for wireless power transfer with repeater

$$k_{\mathrm{e}0} = \frac{R_0}{\omega_0 L_0} = \sum_{j=1}^{j=m} k_{\mathrm{e}0,j} \tag{27}$$

Where $k_{\mathrm{e}0,j}$ is the external coupling coefficient of the transmitter ($k_{\mathrm{e}0}$) distributed to jth receiver. According to (16), the percentage of power received by jth receiver will be:

$$\%P_j \mid_{j=1 \ to \ m} = \frac{k_{\mathrm{e}0,j}}{k_{\mathrm{e}0}} \times 100\% \tag{28}$$

Finally, external coupling coefficient of each receiver has to be:

$$k_{\mathrm{e}j} \mid_{j=1 \ to \ m} = {k_{\mathrm{e}0,j}}^{(-1)^{n(j)}} \times \prod_{i=1}^{i=n(j)} {k_{ij}}^{2(-1)^{i+n(j)}} \tag{29}$$

Where $k_{\mathrm{e}j} \mid_{j=1 \ to \ m}$ is realized using impedance inverters with characteristic impedance:

$$K_{\mathrm{e}j} \mid_{j=1 \ to \ m} = \sqrt{k_{\mathrm{e}j} \omega_0 L_{n(j)j} R_{\mathrm{L}j}} \tag{30}$$

III. Simulation Result

Calculation and simulation results of multi-receiver and repeater are given in this section to demonstrate the proposed power division method. The equivalent circuit of a two-receiver system and with one repeater inserted between the first receiver and the transmitter is simulated using LTspice. Fig. 9 shows the simulation circuit after implementing impedance transformation at both receiver. The element values of the system are listed below:

$$\begin{aligned} \omega_0 &= 2\pi \times 13.56\,\mathrm{MHz} \\ L_0 &= L_{11} = L_{21} = L_{12} = 9.4\,\mu\mathrm{H} \\ C_0 &= C_{11} = C_{21} = C_{12} = 14.7\,\mathrm{pF} \\ R_0 &= R_{\mathrm{L}1} = R_{\mathrm{L}2} = 50\,\Omega \\ k_{11} &= k_{21} = 0.066 \\ k_{12} &= 0.084 \end{aligned} \tag{31}$$

The internal resistance of all the resonant coils are set to $1\,\Omega$ and the internal resistance of inductors in inverter circuits are set to $0.5\,\Omega$. The power ratio $P_1 : P_2$ for this first

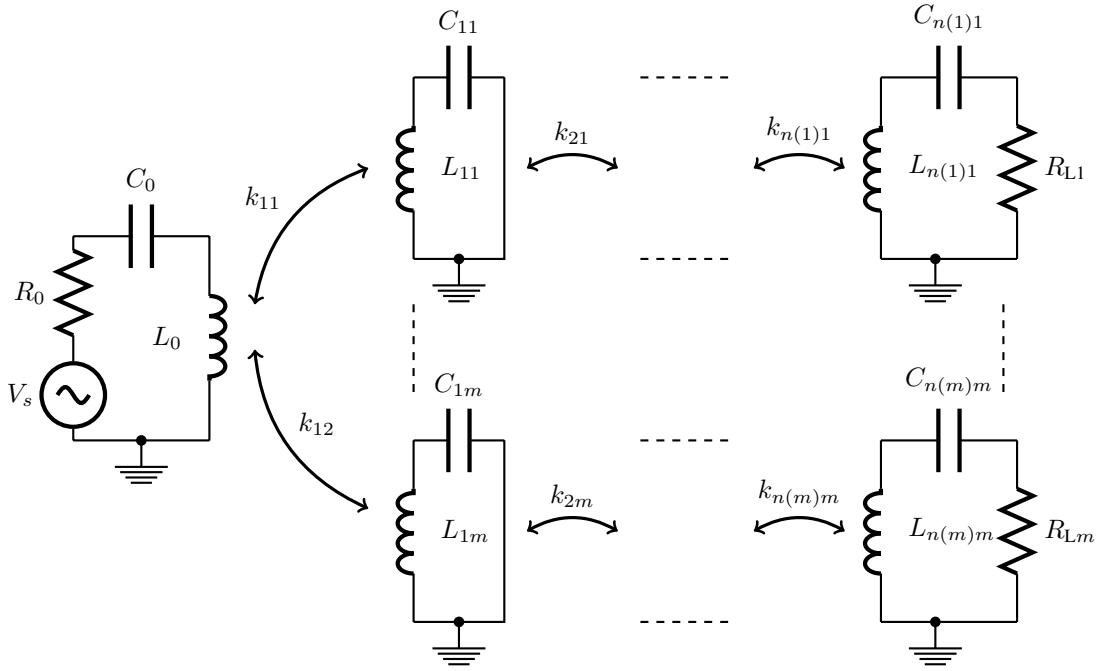

Fig. 8. Wireless power transfer with arbitrary number of receivers and repeaters

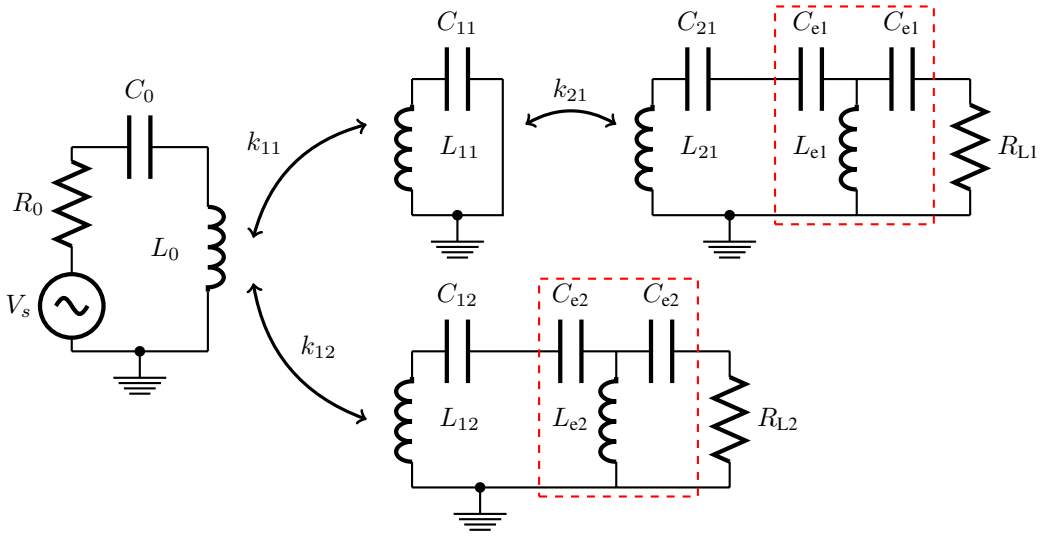

Fig. 9. Simulation circuit

simulation is set to 1, where P_1 is the power received by load R_{L1} and P_2 is the power received by load R_{L2}. Using (27) to (30):

$$\begin{aligned} k_{\mathrm{e}0} &= 0.062 \\ k_{\mathrm{e}0,1} &= k_{\mathrm{e}0,2} = 0.031 \\ k_{\mathrm{e}1} &= 0.031 \\ k_{\mathrm{e}2} &= 0.225 \\ K_{\mathrm{e}1} &= 35\,\Omega \\ K_{\mathrm{e}2} &= 95\,\Omega \end{aligned} \tag{32}$$

Using (7), the element values in the impedance inverter circuits inside dashed rectangular of Fig. 9 are:

$$\begin{aligned} C_{\mathrm{e}1} &= 335\ \mathrm{pF} \\ L_{\mathrm{e}1} &= 0.41\ \mu\mathrm{H} \\ C_{\mathrm{e}2} &= 126\ \mathrm{pF} \\ L_{\mathrm{e}2} &= 1.1\ \mu\mathrm{H} \end{aligned} \tag{33}$$

Fig. 10(a) shows the simulation result before applying the method. Due to impedance mismatch, the reflection ratio, η_{11} is around 22% at the resonant frequency 13.56 MHz. The transmission ratio, η_{21} to the first receiver, which is separated with the transmitter by a repeater coil is around 27%. The transmission ratio, η_{31} to the second receiver is around 48%. The simulation result after inserting inverter

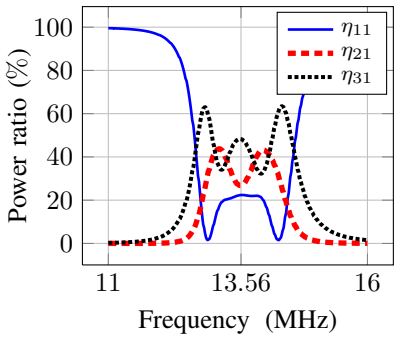

(a)

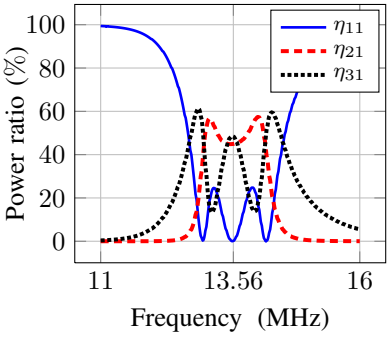

(b)

Fig. 10. Simulation result of equal power division: a) before method b) after method

circuits with characteristic impedance calculated above is shown in Fig. 10(b). Reflection ratio is reduced to almost none, and both receivers obtain almost equalized power as desired.

In the second simulation, power ratio $P_1 : P_2$ is set to be $\frac{7}{3}$. Using the same calculation steps as the previous simulation case, the characteristic impedance of the inverters and element values are:

$$\begin{aligned} K_{e1} &= 42\,\Omega \\ K_{e2} &= 122\,\Omega \\ C_{e1} &= 281\text{ pF} \\ L_{e1} &= 0.49\,\mu\text{H} \\ C_{e2} &= 96\text{ pF} \\ L_{e2} &= 1.43\,\mu\text{H} \end{aligned} \tag{34}$$

Fig. 11 shows the simulation result after applying the method. Similar to equal power distribution case, reflection ratio, η_{11} is reduced to almost none. Transmission ratio, η_{21} to the first receiver is around 64% and transmission ratio, η_{31} to the second receiver is around 29% as desired.

IV. Experiment Results

Experiments are performed for the simulation cases discussed in the previous section. The experiment setup is shown in Fig. 12. The equipment used is Agilent Technologies vector network analyzer E5061B (VNA). All the coils are open type helical, 150 mm in radius, 5 mm in pitch,

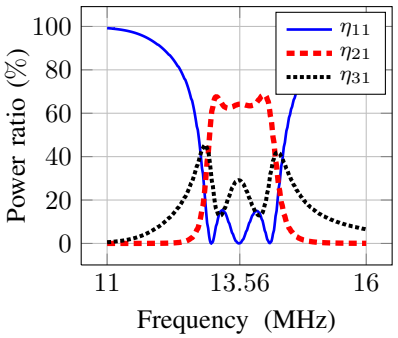

Fig. 11. Simulation result of 70%-30% power division

five copper wire turns and with internal resistance around $1\,\Omega$. They are tuned to resonate at (13.56 ± 0.01) MHz. Transmitter, repeater and first receiver are arranged side by side horizontally. The second receiver is placed 16 cm vertically above the transmitter. Coupling coefficients and coils' approximated measurements are the same as the values given in the simulation result section. Port-1 of VNA which acts as source is connected to the transmitter. One receiver is connected to the port-2 of the VNA at a time to measure the power received. The other receiver is terminated by a RF $50\,\Omega$ terminator as shown in Fig. 13. When measuring reflection coefficient, S_{11}, both receivers are terminated by RF $50\,\Omega$ terminator. Reflection coefficient, S_{11} and forward gain, S_{21} are then recorded from the VNA. The reflected power ratio η_{11}, power ratio for the first receiver η_{21}, and power ratio for the second receiver η_{31} are then calculated:

$$\begin{aligned} \eta_{11} &= |S_{11}|^2 \times 100\% \\ \eta_{21} &= |S_{21}|^2 \times 100\% \\ &\quad \text{(first receiver connected to port-2)} \\ \eta_{31} &= |S_{21}|^2 \times 100\% \\ &\quad \text{(second receiver connected to port-2)} \end{aligned} \tag{35}$$

Plot in Fig. 14(a) shows the frequency response before applying method. At 13.56 MHz, reflected power η_{11} is 23%, η_{21} is 25% and η_{31} is 48%. Impedance transformation is applied at both receivers for impedance matching and equal power division. The capacitors in the inverter circuit shown in Fig. 13 are ceramics capacitors and the inductor is ferrite core wounded with cooper wires. The internal resistance of the inductors are measured to be around $0.5\,\Omega$. The capacitance and inductance chosen are close to the calculated values in (33). The plot in Fig. 14(b) shows that the reflection ratio,η_{11} is reduced to around 4%, while η_{21} is 38% and η_{31} is 49% after implementing proposed method.

In the second experiment, inverters with capacitance and inductance values listed in (34) are implemented in both receivers to obtain $P_1 : P_2$ ratio of $\frac{7}{3}$. Reflection ratio, η_{11} is reduced to around 5%. Transmission ratio, η_{21} to the first receiver is around 55% and transmission ratio, η_{31} to the second receiver is around 31%.

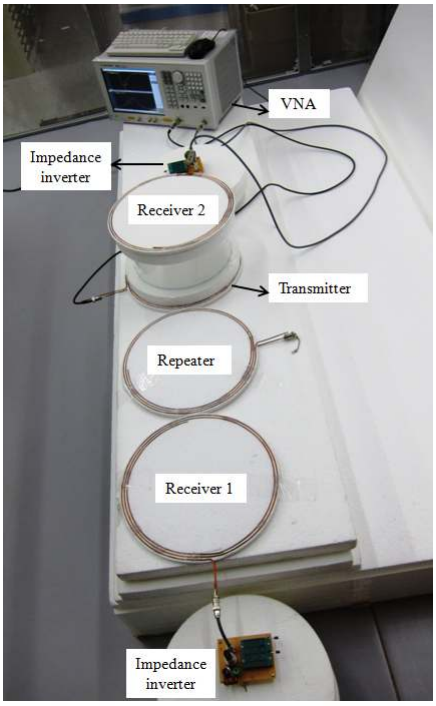

Fig. 12. Experiment Setup

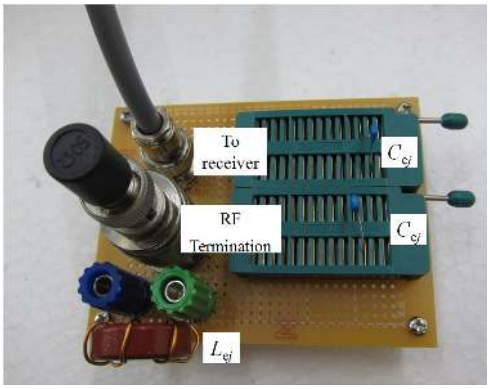

Fig. 13. Inverter circuit

Table I shows the summary simulation and experiment result of the system at the frequency of interest, 13.56 MHz. From simulation result, first receiver will suffer more loss as there is an additional repeater loss compared to second receiver. There are maybe other non-ideal parameters that cause low η_{21} values compared to calculation. In all experiment cases, the higher reflection coefficients compared to the simulation results may be due to different connector interface used in VNA calibration from the connector interface used in actual measurement and the resonator coils do not have perfect 13.56 MHz resonant frequency.

V. Discussion

A. Dissipation Loss in Coils

As can be seen in both the simulation and experiment results at 13.56 MHz, loss occurs in the system. Assuming the loss is caused by heat dissipation in internal resistance

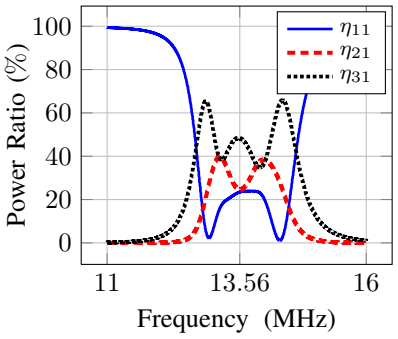

(a)

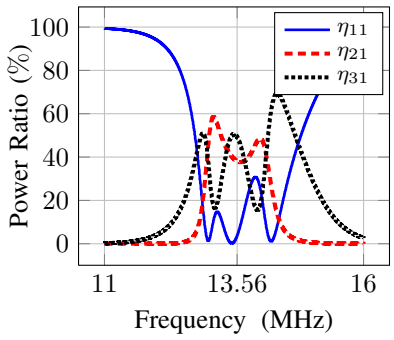

(b)

Fig. 14. Experiment result of equal power division: a) before method b) after method

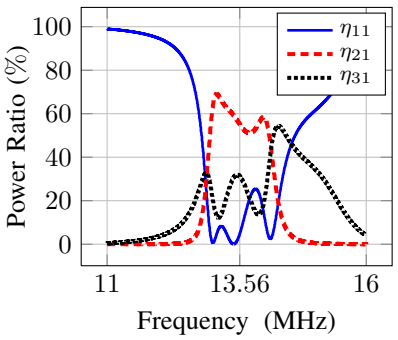

Fig. 15. Experiment result of 70%-30% power division

TABLE I
Simulation and Experiment Results at 13.56 MHz

	Simulation	Experiment
Before Method		
η_{11}	22%	23%
η_{21}	27%	25%
η_{31}	48%	48%
After 50%-50% division		
η_{11}	0%	4%
η_{21}	45%	38%
η_{31}	48%	49%
After 70%-30% division		
η_{11}	0%	5%
η_{21}	64%	55%
η_{31}	29%	31%

TABLE II
LOSS IN COILS FOR THE 50%-50% DIVISION SYSTEM

	Percentage loss
η_0	1.9%
η_{11}	0.4%
η_{21}	1.9%
η_{12}	0.6%
η_{e1}	1.4%
η_{e2}	0.6%
Total	6.8%

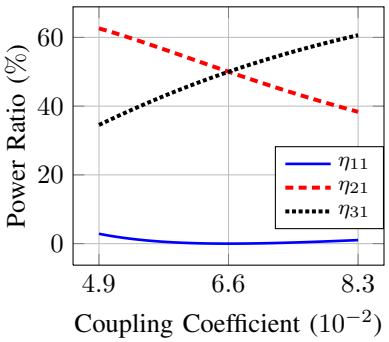

Fig. 16. Method sensitivity toward coupling variations

of coils in resonators and inverter circuits, and this internal resistance is in series with the coils. The loss can then be calculated using square of magnitude current flowing through the coils multiplied by internal resistance, $|I|^2 r$. Further assuming that the dissipation loss in capacitors is small and can be ignored, we can estimate where the bulk of loss is coming from by using the current measurement in simulations where the resonators coils are estimated to be having $1\,\Omega$ resistance and the inductors in inverter circuits are having $0.5\,\Omega$ resistance. Table II shows the percentage loss in all coils including the coils in inverter circuits for the 50%-50% case.

B. Sensitivity towards Coupling Variations

In actual applications, the position of transmitter and repeaters installed will be fixed. The coupling coefficient towards receiver however will vary each time the receiver is placed. A preliminary study of the proposed method's sensitivity towards small coupling variations is provided in this section. Using the 50%-50% case, plot in Fig. 16 shows the reflection coefficient, and percentage power received by both receivers when coupling coefficient, k_{21} is varying linearly from 0.049 to 0.083. Within the coupling coefficient range, reflection ratio is below 3%. However power received by each receiver varies from 30% to 60%.

C. Sensitivity towards Component Variations

Proposed method offers a simple and fast calculation method for impedance matching and power division for wireless power transfer consist of multiple repeaters and receivers. In real implementation however, exact element values do not exist. A Monte Carlo simulation is performed to investigate the sensitivity of the proposed method towards component variations. Again the 50%-50% case is used as example. Assuming the components are normally distributed, with means given by the derived components formulas and with standard deviations σ such that at least a proportion of p=99% falls within the component tolerance. All the components at the second receiver are fixed. One of the capacitor in inverter of first receiver is simulated with tolerance 25% for three inductor values, the nominal value 0.41 μH and $\pm$25% from the nominal value.

Fig. 17(a) shows the distribution of reflected power ratio for 1000 samples of capacitors. For all three inductor values, the reflection is below 5%. As for the power distribution, an obvious pattern can be seen from 17(b) and 17(c). Increasing the inductance in the inverter circuit increases the impedance viewed towards first receiver. However this change has less impact on the reflection coefficient compared to power division between the two receivers. The distribution of the reflected power and power division for each inductor value only spread slightly from the mean value with 0.33 μH showing the most dispersion.

Applying auto-tuning on the method depends on the requirement of each application. High frequency relays [7] can be used to switch between blocks of inverter circuits installed at the receiver sides. From the Monte Carlo simulation result, the inductor used in actual applications can be built with tighter tolerance and capacitors within $\pm$25% tolerance is acceptable for the method. If high accuracy of power division ratio is required, a finer auto-tuning circuit can be built. Reflection coefficient on the other hand, is more robust towards coupling variations and component variations.

VI. CONCLUSION

New impedance matching and power division method is proposed and generalized for arbitrary number receivers and arbitrary number of repeaters. Due to uniform equations resulted when using impedance inverter representation, the design equations are simple. Impedance matching and power division conditions are in terms of coupling coefficient which is the commonly used representations. In order to implement controllable power division without having to change the coils' position, the external coupling coefficients of the receivers can be modified by inserting impedance inverter circuit in between receiver and the corresponding termination resistor.

REFERENCES

[1] A. P. Sample, D. A. Meyer, and J. R. Smith, "Analysis, experimental results, and range adaptation of magnetically coupled resonators for wireless power transfer," *IEEE Trans. Ind. Electron.*, vol. 58, no. 2, pp. 544-554, Feb. 2011.

[2] K. E. Koh, T. C. Beh, T. Imura, and Y. Hori "Novel band-pass filter model for multi-receiver wireless power transfer via magnetic resonance coupling and power division," *2012 IEEE 13th Annu. Wireless and Microwave Technology Conf. (WAMICON)*, pp. 1-6.

[3] B. L Cannon, J. F. Hoburg, D. D. Stancil, and S. C. Goldstein, "Magnetic resonant coupling as a potential means for wireless power transfer to multiple small receivers," *IEEE Trans. Power Electron.*, vol. 24, no. 7, pp. 1819-1825, Jul. 2009.

[4] A. Kurs, R. Moffatt, and M. Soljacic, "Simultaneous mid-range power transfer to multiple devices," *Appl. Physics Lett.*, vol.96, no.4, pp. 044102-044102-3, Jan. 2010.

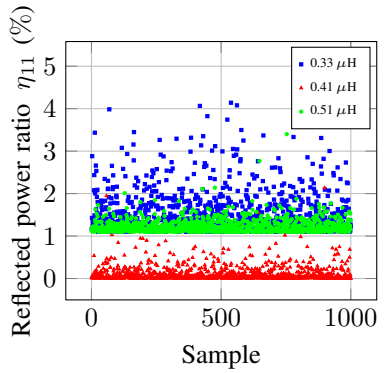

(a)

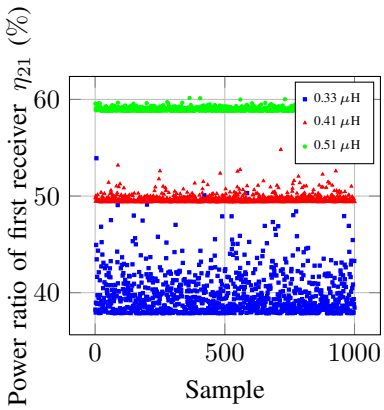

(b)

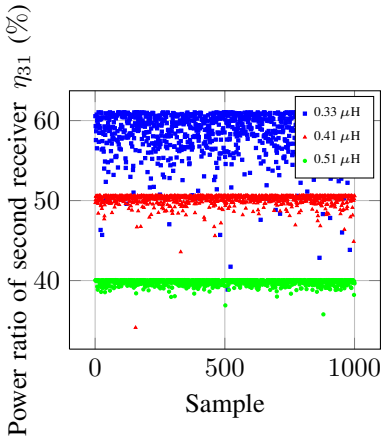

(c)

Fig. 17. Power distribution for 25% component tolerance: a) reflected power ratio, b) power ratio of the first receiver, c) power ratio of second receiver

[5] J. W. Kim, H. C Son, D. H. Kim, K. H. Kim and Y. J. Park, "Analysis of wireless energy transfer to multiple devices using CMT," *2010 Asia-Pacific Microwave Conf. Proc. (APMC)*, pp. 2149-2152.

[6] T. Imura, "Study on maximum air-gap and efficiency of magnetic resonant coupling for wireless power transfer using equivalent circuit," *IEEE Int. Symp. Ind. Electron. (ISIE 10)*, pp. 3664-3669.

[7] T. Beh, M. Kato, T. Imura, S. OH, and Y. Hori, ''Automated impedance matching system for robust wireless power transfer via magnetic resonance coupling,'' *IEEE Trans. Ind. Electron*., vol. 60, no. 9, pp.3689-3698, Sep. 2013.

[8] T. Imura and Y. Hori, "Maximizing air gap and efficiency of magnetic resonant coupling for wireless power transfer using equivalent circuit and neumann formula," *IEEE Trans. Ind. Electron.*, vol. 58, no. 10, pp. 4746-4752, Oct. 2011.

[9] M. Dionigi and M. Mongiardo, "CAD of efficient wireless power transmission systems," *IEEE MTT-S Int. Microwave Symp. Dig. (MTT)*, pp. 1-4.

[10] S. Cheon, Y. H Kim, S. Y. Kang, M. L. Lee, J. M. Lee and T. Zyung, "Circuit-model-based analysis of a wireless energy-transfer system via coupled magnetic resonances," *IEEE Trans. Ind. Electron.*, vol. 58, no. 7, pp. 2906-2914, Jul. 2011.

[11] F. Z. Shen, W. Z. Cui, W. Ma, J. T. Huangfu and L. X. Ran, "Circuit analysis of wireless power transfer by "coupled magnetic resonance"," *IET Int. Communication Conf. Wireless Mobile and Computing (CCWMC 2009)*, pp. 602-605.

[12] I. Awai and T. Komori, "A simple and versatile design method of resonator-coupled wireless power transfer system," *2010 Int. Conf. Communications, Circuits and Systems (ICCCAS)*, pp. 616-620.

[13] I. Awai, T. Komori and T. Ishizaki, "Design and experiment of multi-stage resonator-coupled WPT system," *2011 IEEE MTT-S Int. Microwave Workshop Series on Innovative Wireless Power Transmission: Technologies, Systems, and Applications (IMWS)*, pp.123-126.

[14] J. W. Kim, H. C. Son, K. H. Kim and Y. J. Park, "Efficiency analysis of magnetic resonance wireless power transfer with intermediate resonant coil," *IEEE Antennas Wireless Propag. Lett.*, vol. 10, pp. 389-392, May 2011.

[15] N. Oodachi, K. Ogawa, H. Kudo, H. Shoki, S. Obayashi and T. Morooka, "Efficiency improvement of wireless power transfer via magnetic resonance using transmission coil array," *2011 IEEE Int. Symp. Antennas and Propagation (APSURSI)*, pp. 1707 - 1710.

[16] W. Fu, B. Zhang and D. Qiu, "Study on frequency-tracking wireless power transfer system by resonant coupling," *IEEE 6th Int. Power Electronics and Motion Control Conf.*, pp. 2658-2663.

[17] J. Park, Y. Tak, Y. Kim, Y. Kim and S. Nam, "Investigation of adaptive matching methods for near-field wireless power transfer," *IEEE Trans. Antennas Propag.*, vol. 59, no. 5, pp. 1769-1773, May 2011.

[18] T. Imura and H. Yoichi, "Optimization using transmitting circuit of multiple receiving antennas for wireless power transfer via magnetic resonance coupling," *2011 IEEE 33rd Int. Telecommunications Energy Conf. (INTELEC)*, pp. 1-4.

[19] C. Ma, X. Zhu, and M. Fu, "Wireless charging of electric vehicles: A Review and Experiments," in *ASME 2011 Int. Design Engineering Technical Conferences and Computers and Information in Engineering Conf.*, pp. 881-887.

[20] Y. Yokoi, A. Taniya, M. Horiuchi, and S. Kobayashi, "Developement of KW class wireless power transmission system for EV using magnetic resonant method," presented at 1st Int. Electric Vehicle Technology Conference, Yokohama, Japan, 2011.

[21] R. E. Collin, *Foundations for Microwave Engineering,* 2nd ed., NJ:John Wiley and Sons, Inc., 2001.

[22] J. D. Irwin , R. M. Nelms, *Basic Engineering Circuit Analysis.* 10th ed., NJ:John Wiley & Sons, Inc., 2010.

[23] A. Karalis, J. D. Joannopoulos, and M. Soljacic, "Efficient Wireless Non- Radiative Mid-Range Energy Transfer," *Ann. Phys.*, Vol. 323, No. 1, pp. 34-38, Jan. 2008.

[24] G. L. Matthaei, L. Young, and E. M. T. Jones, *Microwave Filters, Impedance Matching Networks and Coupling Structures*. Norwood, MA: Artech House, 1980.

[25] S. H. Lee and R. D. Lorenz, "Development and validation of model for 95% efficiency, 220 W wireless power transfer over a 30cm air-gap," *2010 IEEE Energy Conversion Congress and Exposition (ECCE)*, pp. 885-892.

[26] Z. N. Low, J. J. Casanova, and J. Lin, "A loosely coupled planar wireless power transfer system supporting multiple receivers," *Adv. Power Electron.*, vol. 2010, pp. 1–13, Mar. 2010.